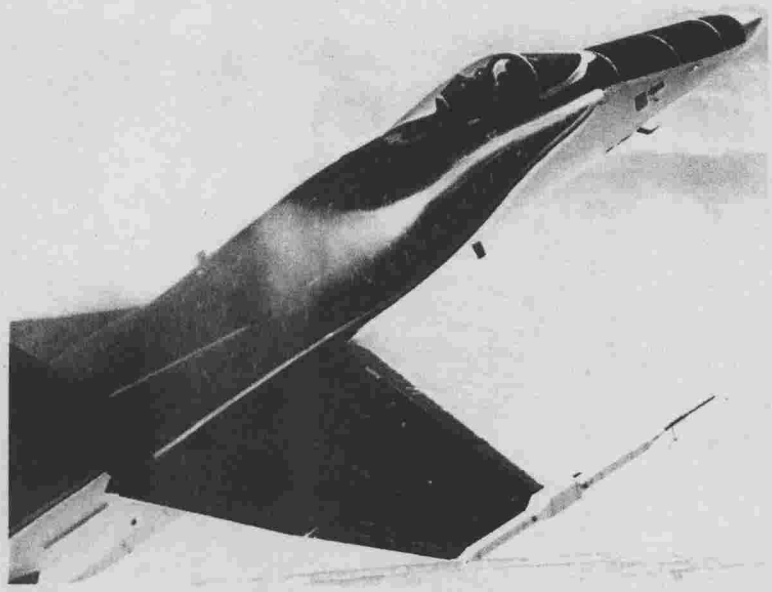

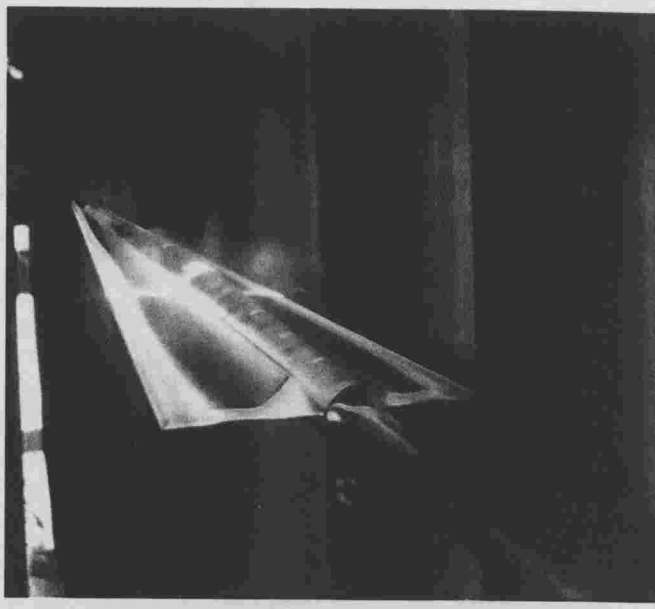

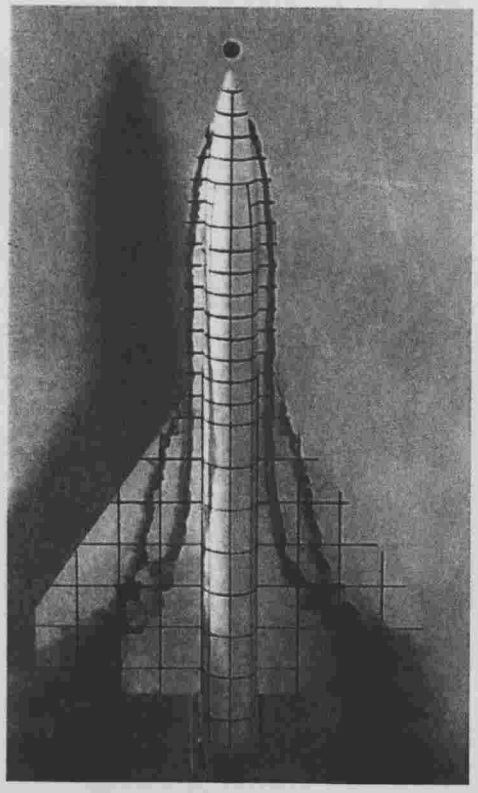

USAF WRIGHT LABORATORY

ICIASF '95

FLIGHT DYNAMICS DIRECTORATE

RECORD

INTERNATIONAL CONGRESS ON
INSTRUMENTATION IN AEROSPACE
SIMULATION FACILITIES

95-CH3482-7

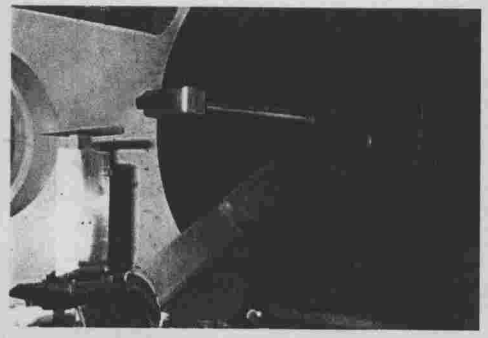

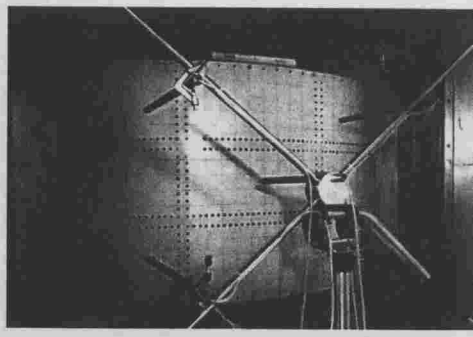

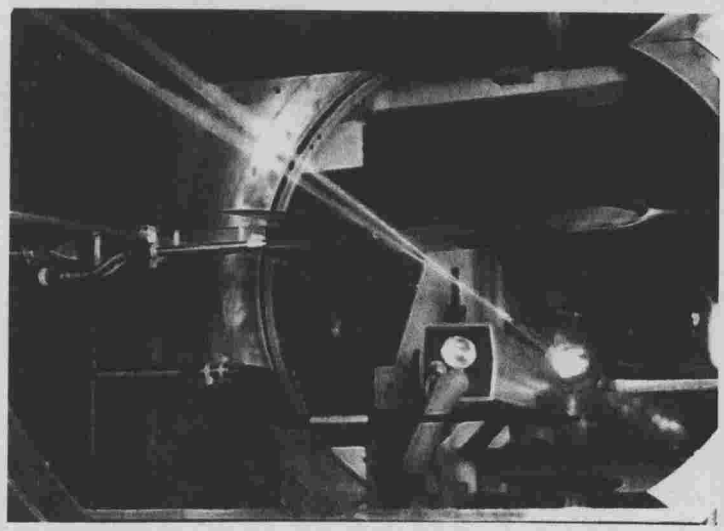

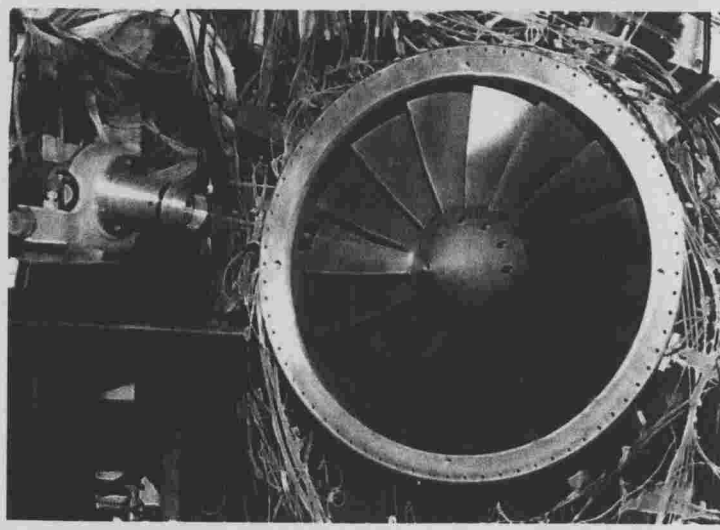

Instrumentation Techniques of the Aachen Shock Tunnel TH2

H. Olivier, H. Grönig

Shock Wave Laboratory, RWTH Aachen
Templergraben 55
52056 Aachen, Germany

with appendix of B. Schulze,
Daimler-Benz Aerospace, Munich, Germany

Abstract: High enthalpy short-duration facilities are mainly used to simulate the hypersonic flow during a reentry into an atmosphere. The special operational features of these facilities put somewhat different requirements on the instrumentation as usual supersonic or hypersonic blow down tunnels. The short running times of the order of some milliseconds require sensors with a very fast response and rise time. To avoid time lags by tubings, usually the sensors are installed flash into the model wall or in a very short distance behind it. This implies that they have to withstand the impact of small particles of high energy, which are transported by the flow. This is the most important reason why for heat flux measurements at severe flow conditions very robust coaxial thermocouples are used. To allow also for a pressure measurement almost at the same location a pressure tap is drilled through the thermocouple. From the measurement of the stagnation point heat flux and the Pitot pressure some information can be found about the free stream. More detailed free stream measurements are possible with a mass flux gauge and a static pressure probe. Due to their complexity the development of these gauges require intensive testing and the support of numerical calculations. The same holds for the development of a force balance which meets the requirements of a shock tunnel application.

INTRODUCTION

The development of modern reentry vehicles requires extensive testing in hypersonic facilities. The results achieved are used for the design process as well as for CFD-code validation. The experimental facilities cover a range from conventional blow down tunnels with flow velocities of about 1 km/s to short-duration facilities like shock tunnels and free piston driven shock tunnels with maximum flow velocities of about 8 km/s. In most of these tunnels pressure and heat flux measurements are performed at the model surface, as well as integral measurements of the aerodynamic forces and moments.

The present paper gives an overview of the instrumentation techniques used at the Aachen shock tunnel TH2. The special features of a shock tunnel, short running times in the order of a few milliseconds and stagnation temperatures of several thousand degree, place high demands on the instrumentation. Pressure and heat flux as well as force and moment measurements are performed. To make these results comparable to others, nondimensional pressure, force and moment coefficients as well as Stanton numbers are deduced. This requires the knowledge of the free stream conditions, which in particular for shock tunnels are somewhat difficult to determine. In this paper two methods will be described to yield the free stream mass flux; from the stagnation point heat flux of a sphere the total enthalpy of the flow is deduced, and a static pressure probe, which is in development, will allow to measure the static pressure of the free stream.

With a fast infrared camera it was possible to demonstrate the feasibility of this technique for short-duration, impulse facilities. With this camera it was possible to take a 2-d picture of 128 x 128 pixels each millisecond. First results of these tests are presented in the appendix of this paper.

The short running times of a shock tunnel pose a big problem for force and moment measurements, because the lowest natural frequency of a usual wind tunnel balance is too low, so that the balance is not able to follow the temporal evolution of the forces and their steady phase. Therefore, for shock tunnel applications a special balance has been designed which meets these requirements. The results achieved with this balance installed into a cone model show a good agreement with theoretical ones and confirm the reliability of the force measuring technique employed.

HEAT FLUX MEASUREMENTS

Thin Film Gauges

The methods available for temperature and heat flux measurement in short-duration hypersonic facilities have been comprehensively reviewed by Schultz and Jones in 1973 [1]. As during the short test time the surface temperatures of the models do not reach the high levels that occur with the real vehicle during flight, the temperature itself is of minor interest. The

CH34827-95/0000-01.1 $1.00©1995 IEEE

heat flux is a more meaningful quantity which can easily be simulated and remains constant during the test time in the shock tunnel. To derive the heat flux from a surface temperature measurement, one needs a mathematical relation connecting both quantities. Taking into account one-dimensional heat conduction into a semi-infinite slab only, one obtains a straightforward solution [1, page 7]:

$$\dot{q}_s = \sqrt{\frac{\rho c k}{\pi}} \left[\frac{T(t)}{\sqrt{t}} + \frac{1}{2} \int_0^t \frac{T(t) - T(\tau)}{(t-\tau)^{3/2}} d\tau \right] , \qquad (1)$$

where $\dot{q}$ denotes the heat flux through the surface; ρ the density, c the specific heat, k the thermal conductivity of the semi-infinite slab; T the surface temperature; t the time and τ the integration variable.

If the surface temperature of the semi-infinite slab is measured and digitalized as a function of time and the properties ρ, c and k of the substrate are known, then the heat flux through the surface can be computed using equation (1). The application of this principle requires a surface temperature sensor with a homogeneous backing material and a sensing element of negligible thickness and mass. Thin film resistance thermometers meet these requirements and are being used since decades though problems have always been present with contacting the film and scaling down the sensors. Two platinum wires sintered into a cylindrical ceramic substrate helped to overcome both problems [2]. Figure 1 shows the construction of the substrate and three sensors ready for use.

Zirconium oxide (ZrO_2) has qualified as a suitable substrate material due to its high tensile strength (1082 MPa), ductility (breaking elongation $4.5 \cdot 10^{-3}$) and low thermal conductivity ($2.5 \frac{W}{mK}$). Particularly, the low thermal conductivity is necessary to simulate a semi-infinite slab also with a small substrate and to achieve a high surface temperature leading to a high signal output. The sensing element is a nickel or platinum film that serves as temperature sensitive resistor. It is deposited on the previously polished substrate by means of vacuum evaporation of the metal. The shape of the film is determined by a mask that is produced on the surface of the substrate in a photomechanic step employing light sensitive laquer. Thereby a certain freedom in the choice of the film geometry is guaranteed, that allows for adjusting the sensitivity of the sensor – which is proportional to the film length – to the current demands. These new sensors resisted many shock tunnel experiments in different models and are in permanent use. Should a sensor be destroyed, the substrate can be reused by

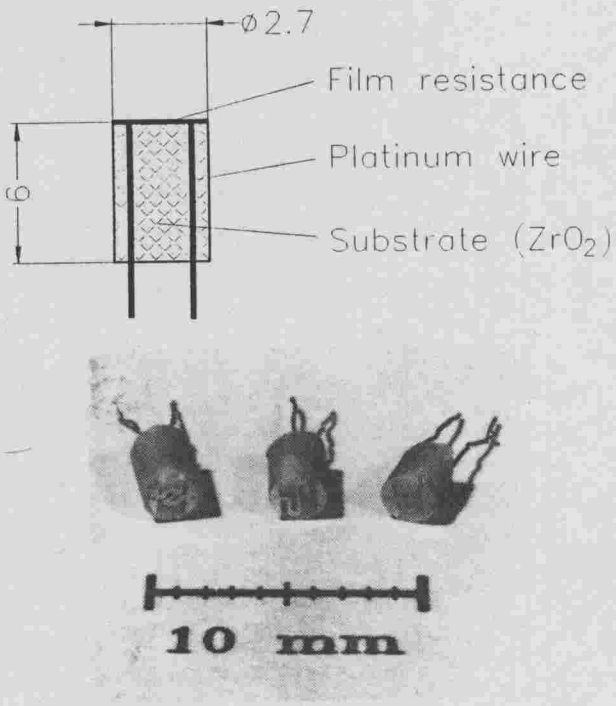

Fig. 1: Thin film gauges

polishing it again and making a new sensor with a new film. The contacting of the film is conveniently accomplished by the platinum wires leading through the substrate to the surface. During the experiment the sensor is supplied with a constant current of 7 mA, so that the voltage is porportional to the resistance of the film and consequently to the temperature.

Coaxial Thermocouple with Simultaneous Pressure Measurement

It is well known that thin-film resistance thermometers are not able to withstand the rough conditions of the hypersonic flow at locations around a model where high heat fluxes are generated. Therefore thin film thermometers are only used at locations of the model where the heat fluxes are relatively low and the flow conditions not too severe. At locations of the model where high heat fluxes occur, like stagnation or reattachment regions after flow separation, thermocouples are used. These gauges are very robust and able to withstand highly severe flow conditions. Of course the sensitivity of thermocouples is much less than that of thin-film resistance thermometers. But this is not important because thermocouples are mainly used in regions of high heat fluxes. Therefore the combined use of thin-film resistance thermometers for low heat fluxes and of thermocouples for high heat fluxes gives an optimum of accuracy and repeatability for the heat flux measurements.

Based on already available coaxial thermocouples, a probe has been designed which allows a surface temperature and pressure measurement almost at the same location (spatial deviation between temperature and pressure measurement 1.5 mm). It comprises all the features of commercial coaxial thermocouples, like fast response time (some microseconds), very robust, through-the-wall mounting technique, adaption to the wall surface shape, forming of the junction by filing or by vacuum deposition of a metallic coating.

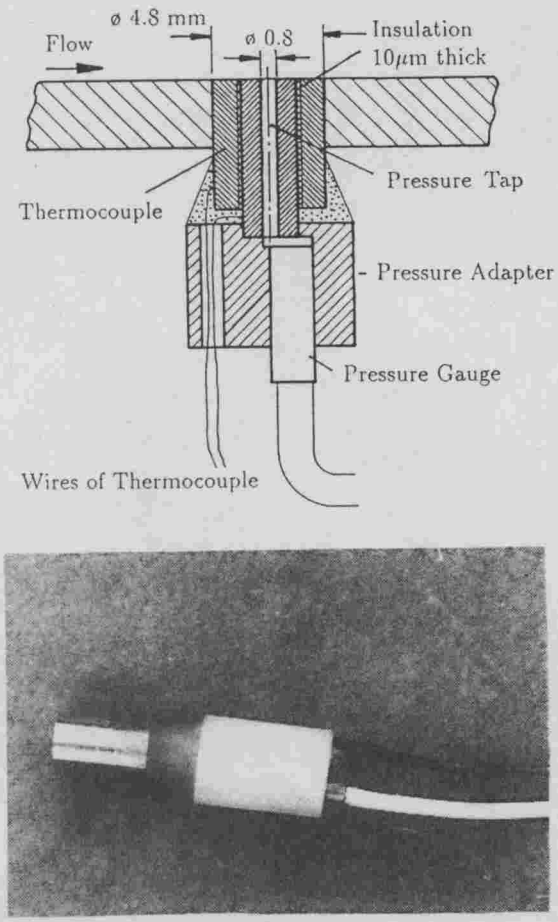

Fig. 2.: Coaxial thermocouple with integrated pressure gauge

The thermocouple consists of a center wire which fits into a tube. These form the two legs of the thermocouple which are isolated by a 10 μm thin dielectric (see Fig. 2). Through the inner element of the thermocouple a pressure hole is drilled which via an adapter is connected to a pressure gauge. The outer diameter of the thermocouple amounts to 4.8 mm and the diameter of the inner element is 3.0 mm. These dimensions have been chosen in order to fulfill the operational requirements of an impulse facility, i.e. during a maximum measuring time of 10 ms the temperature measurement is not disturbed by radial heat fluxes emerging from the pressure tap or the junction between the model surface and the outer thermocouple element. The thermocouple materials are chromel for the tube and constantan for the center element (Typ E). Commercial pressure transducer like Kulite, Endevco, etc. are mounted into the pressure adapter.

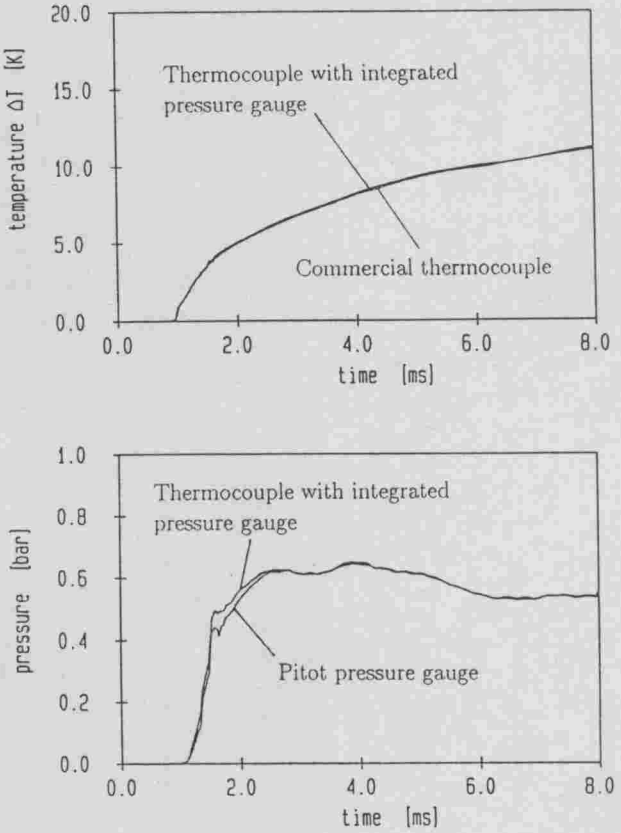

Fig. 3: Temperature and pressure signals of the coaxial thermocouple, tested in the shock tunnel TH2, $M_\infty = 7$, $T_0 = 1500$ K

Figure 3 shows a comparison of the temperature and pressure signal achieved by the coaxial thermocouple with pressure tap, a Pitot pressure gauge, and a commercial thermocouple, which were installed separately in the test section of the shock tunnel. The temperature and pressure signals are almost identical. In general, deviations in the temperature signal may occur due to different sensitivities and slightly different material properties, which are described by the so-called ρck-value. But a proper calibration of the sensitivity and the thermal properties ρck accounts for the deviations in the temperature signals of different probes, so that for the same flow condition the same heat flux is achieved.

The ρck-value of the thermocouple is determined by a method, where the thermocouple is dipped into a heated fluid with known ρck-value. With the help of the one-dimensional heat conduction theory a simple relation can be derived, which allows to determine the unknown ρck-value of the thermocouple as function of the initial temperature of the fluid T_{FL}, of the thermocouple T_{TC}, the contact temperature T_C, which is measured by the thermocouple, and the known ρck-value of the heated fluid [2]:

$$(\rho ck)_{TC} = (\rho ck)_{FL} \frac{T_C - T_{FL}}{T_{TC} - T_C}. \qquad (2)$$

The sensitivity of the thermocouple is determined by a static calibration. With the coaxial thermocouple installed at the stagnation point of a sphere with 25 mm diameter heat fluxes of about 1200 W/cm^2 have been measured.

DETERMINATION OF FREE STREAM CONDITIONS

In most of the hypersonic facilities at the model surface pressure and heat flux as well as integral measurements, like force and moment measurements, are performed. These absolute values strongly depend on the flow conditions, therefore they are transformed into nondimensional expressions, like pressure coefficient, Stanton number etc., to allow for a comparison with results achieved for different flow conditions. This requires the knowledge of the free stream conditions, which, due to their special operational characteristics in the case of shock tunnels, are somewhat difficult to determine. Nevertheless, in the following, methods are described to determine the total enthalpy of the flow, which allows to estimate the free stream velocity and to measure the free stream mass flux and the static pressure.

Classical Method

In conventional hypersonic wind tunnels with long running times and relatively low stagnation temperatures the free stream conditions can be determined quite accurately by a nozzle flow calculation which as input only needs the reservoir conditions. But for short-duration facilites, which produce much higher flow velocities connected with much larger stagnation temperatures, the situation is more complex. In this case the determination of the free stream conditions by a nozzle flow calculation is accompanied by a number of uncertainties. These arise due to several problems:

- owing to the complex shapes of the reflected shock at the shock tube end wall, a reliable computation of the reservoir temperature, which has to be known for the nozzle flow calculation, is not possible, in addition, caused by radiation and driver gas contamination the influence of heat losses is unknown,
- the computation of the nozzle flow is not very reliable because of unreal chemical and thermal models of the nozzle flow, and also due to an uncertain description of the transitional and turbulent nozzle boundary layer,
- using the measured pressure of the nozzle reservoir and the Pitot pressure in the test section for a nozzle flow calculation, in short-duration facilities, one has to take into account the time delay caused by the finite signal travelling speed between the reservoir and the test section. This time delay cannot be predicted accurately.

To overcome these problems and thus to increase the accuracy of the experimental results, one mainly makes use of input data, which are measured within the test section proper. The method is based on a Pitot pressure and a heat flux measurement at the stagnation point of a sphere. The theory of Fay and Riddell [3] is employed to achieve the total enthalpy of the flow:

$$\dot{q}_{Stag.} = 0.94\,(\rho_w \mu_w)^{0.1} (\rho_s \mu_s)^{0.4} \left[1 + (Le^{0.52} - 1)\frac{h_D}{h_s}\right] \cdot (h_s - h_w) \left(\left.\frac{du}{dx}\right|_s\right)^{0.5}. \qquad (3)$$

Here Le indicates the Lewis number, all other symbols have their usual meaning. The subscript w denotes the wall conditions and the subscript s the flow conditions of an imaginary stagnation point outside of the boundary layer. For the estimation of the tangential velocity gradient in the past the simple Newtonian approach has been used [3]:

$$\left.\frac{du}{dx}\right|_s = \frac{1}{R}\sqrt{\frac{2(p_s - p_\infty)}{\rho_s}}, \qquad (4)$$

but recently a more sophisticated method has been proposed by Olivier [4], which results in a higher accuracy:

$$\left.\frac{du}{dx}\right|_s \frac{D}{u_\infty} = \frac{2(1+\overline{\Delta})}{\overline{\Delta}} \frac{p_s - p_2}{\rho_\infty u_\infty^2} \frac{\rho_2}{\rho_s}, \qquad (5)$$

with the sphere diameter $D = 2R$, the nondimensional shock stand-off distance $\overline{\Delta} = \Delta/R$ and the pressure p_2 immediately behind the shock.

With this procedure and the measured stagnation point heat flux it is possible to deduce the time history

of the stagnation temperature, as shown in Fig. 4 for various flow conditions.

There, nominal temperatures for frozen and equilibrium flow are also included, which have been determined by a nozzle flow computation. The time histories of the stagnation temperature can be used as one tool to estimate the useful running time of the tunnel.

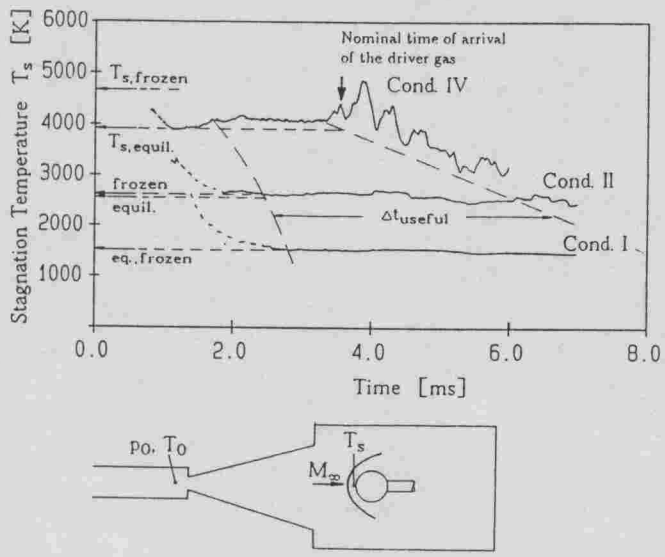

Fig. 4: Time histories of the stagnation temperature for various test conditions

For free stream mass flux and dynamic pressure the following expressions are derived from the normal shock relations [5]:

$$\rho_\infty u_\infty = \frac{p_s}{RT_s}\sqrt{2(h_s - h_\infty)} \cdot \left(1 - \sqrt{1 - \frac{RT_s}{p_s}\frac{p_s - p_\infty}{h_s - h_\infty}}\right) \qquad (6)$$

and

$$\rho_\infty u_\infty^2 = \frac{2p_s}{RT_s} \cdot (h_s - h_\infty)\left(1 - \sqrt{1 - \frac{RT_s}{p_s}\frac{p_s - p_\infty}{h_s - h_\infty}}\right). \qquad (7)$$

Since, generally for hypersonic flows the free stream values p_∞ and h_∞ are much smaller than the Pitot pressure p_s and enthalpy h_s, their influence on the accuracy achieved is negligible. The free stream static pressure p_∞ is either measured at the nozzle exit, or in the free stream with a static pressure probe, as will be presented below, or an approximate value is used. The free stream static enthalpy is expressed as function of the static pressure and free stream density. As it has been shown [5], the expressions deriv are valid for a wide range of flow conditions which a include real gas effects.

Mass Flux Probe

Based on a principle proposed by Stalker [6], a m flux probe has been designed and tested in the Aach shock tunnel. It allows to deduce the free stream m flux avoiding any measurement of hot stagnation c ditions. This is important for high enthalpy facilit because the accurate measurement of hot stagnati conditions very often is not very reliable and acco panied by measuring problems. The schematic rangement of the probe is shown in Fig. 5.

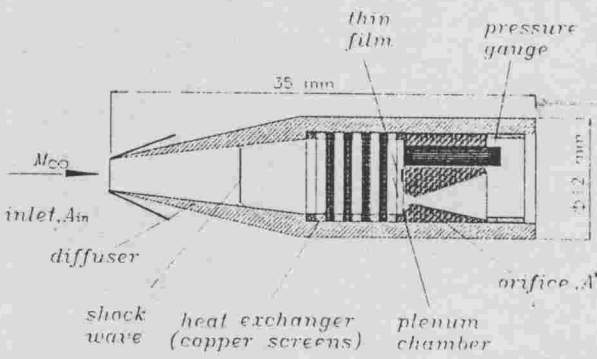

Fig. 5: Schematic arrangement of the mass flux pro

The approaching supersonic flow is captured with a stream tube of cross-sectional area equal to that the intake. This is ensured, if there is no detach shock wave in front of the probe. Inside of it, first t flow expands and then decelerates through a syst of shock waves which are represented as a single n mal shock. After this the hot gas passes through t heat exchanger which cools it down to a value whi ensures ideal gas behaviour, and then ejects throu the orifice at the rear of the probe. If the pressure tio across the orifice is such that there is a sonic flo a measurement of pressure and temperature in t plenum chamber allows the calculation of the ejec mass flow. This can be equated to the mass flow the intake when the probe is operating in the stea state.

Assuming ideal gas behaviour and an isentropic expansion of the gas through the orifice the mass flux can be calculated in the following way [6]:

$$\rho_\infty u_\infty = \frac{p_m}{\sqrt{T_m}} \frac{A^*}{A_{in}} \sqrt{\frac{\gamma}{R}\left(\frac{2}{\gamma+1}\right)^{\frac{\gamma+1}{\gamma-1}}}, \qquad (8)$$

where p_m and T_m are pressure and temperature of the gas within the plenum chamber. A problem arises in the determination of the gas temperature T_m. Stalker assumed, that the effectiveness of the heat exchanger is high enough that for T_m the ambient temperature can be assumed. To overcome this uncertainty the heat flux is measured within the plenum chamber from which the temperature is deduced. This requires the knowledge of the relation between heat transfer, gas temperature and pressure within the plenum chamber. For a fixed geometry of the plenum chamber and ejection orifice the heat flux to the walls of the plenum chamber depends on the gas temperature and pressure. To find this relation we installed the rear part of the mass flux probe, consisting of plenum chamber and ejection orifice, into the end wall of a shock tube. Then experiments were performed with different shock Mach numbers and initial pressures. The heat flux to the rear wall of the plenum chamber as well as the pressure behind the reflected shock were measured, where the last one represents the pressure within the plenum chamber. From this, the temperature behind the reflected shock was computed which, for the calibration tests is equal to the gas temperature within the plenum chamber. In this way tests with temperatures up to 1500 K were performed. In the context of shock tube flow these temperatures are not very high. Therefore their computation from the measured pressures and shock Mach numbers is quite reliable. Figure 6 shows the heat flux data which were achieved within the shock tube. In this case the diameter of the plenum chamber amounts to 5 mm and that of the orifice to 2 mm.

From these calibration results the following relation can be set up between the temperature and pressure within the plenum chamber and the wall heat flux measured during the test:

$$T_m = T_{ref} + 36.4 \frac{\dot{q}_m}{\dot{q}_{ref}} \left[\left(\frac{p_m}{p_{ref}} \right)^{-0.368} - 0.34 \right]. \qquad (9)$$

For the reduction of the mass flux from Eq. (8) it is also important to know the effective orifice area A^*, because the geometrical area is reduced by the displacement thickness of the boundary layer. To account for this effect, one has to calibrate the effective area for different flow conditions. In the calibration tests the mass flux through the probe, as well as the pressure and the temperature in the plenum chamber are known, so that Eq. (8) can be used to determine the effective throat area. A typical result of such a calibration is shown in Fig. 7, where the effective throat diameter is plotted versus the unit Reynolds number of the flow at the throat. The calibration results are approximated by the relation:

$$D_{eff} = 2.05 - 320\sqrt{Re/L} \quad [\text{mm}]. \qquad (10)$$

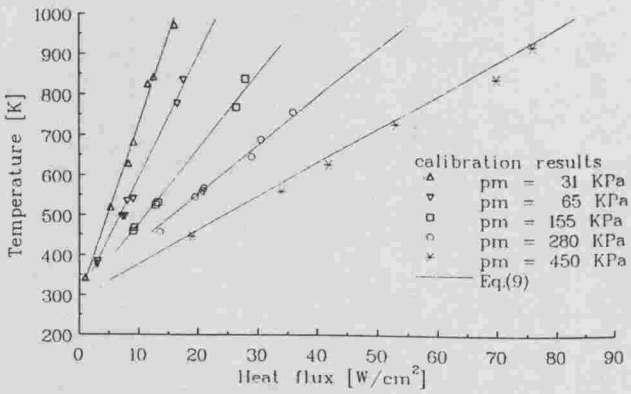

Fig. 6: Calibration results of temperature T_m for a mass flux probe

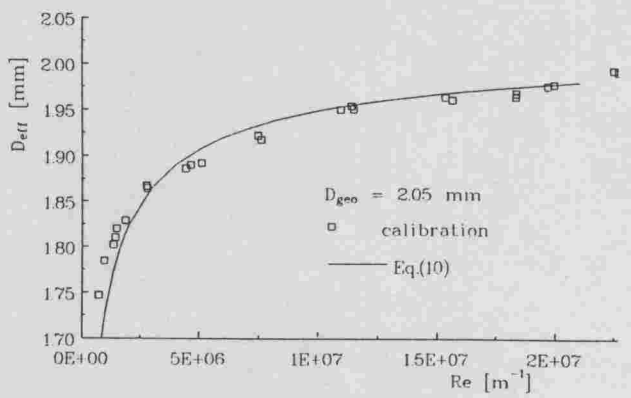

Fig. 7: Influence of the throat Reynolds number on the effective orifice diameter

After calibration, different mass flux probes were tested in the Aachen shock tunnel. Figure 8 shows a comparison of the mass fluxes achieved for a flow of $M_\infty = 7$, stagnation temperature $T_0 = 1500$ K and nozzle reservoir pressure $p_0 = 65$ bar. The agreement between the result of the mass flux probe and that achieved by the classical method described above is very good. In this case, inside of the mass flux probe

a single copper screen was installed, which reduced the flow temperature down to 550 K. The pressure in the plenum chamber was about 1/4 of the Pitot pressure.

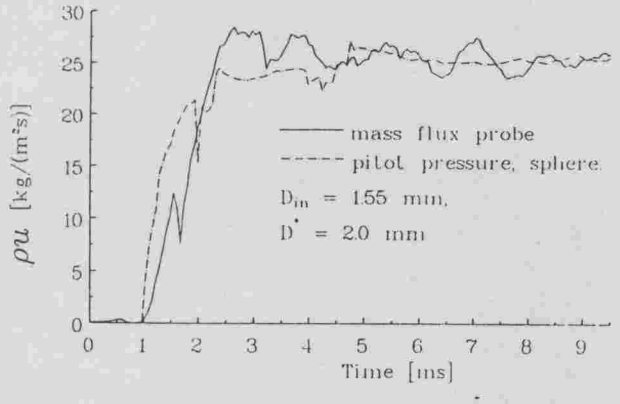

Fig. 8: Free stream mass flux for $M_\infty = 7$, $T_0 = 1500$ K, $p_0 = 65$ bar

Figures 9 to 11 show experimental results of the mass flux probe for $M_\infty = 7$, stagnation temperature $T_0 = 3800$ K and nozzle reservoir pressure $p_0 = 380$ bar. In this case the pressure in the plenum chamber (see Fig. 9) is about 10 % of the Pitot pressure. The gas temperature in the plenum chamber is cooled down from 3800 K to about 700 K. This demonstrates the applicability of the probe also for high enthalpy conditions. The low temperature within the plenum chamber ensures the validity of the mass flux equation (8), and due to the associated high density it helps to capture the shock inside of the probe. The high peak at the beginning of the run is of no physical meaning, because during the flow establishment the pressure is very low and for these low pressures the calibration results of the plenum temperature are not valid.

For this test condition the mass flux slightly increases with time (see Fig. 11). This might indicate a drop of the nozzle reservoir temperature, whereas during this time the nozzle reservoir pressure is more or less constant. In Fig. 11 also nominal mass flux values are indicated, which have been achieved by nozzle flow calculations for both equilibrium as well as frozen conditions. For the quasi-steady period good agreement exists for the mass flux probe and the computed value for equilibrium flow. During this time the deviation between the results of the mass flux probe and that achieved by the Pitot probe and the sphere amounts to 10 %.

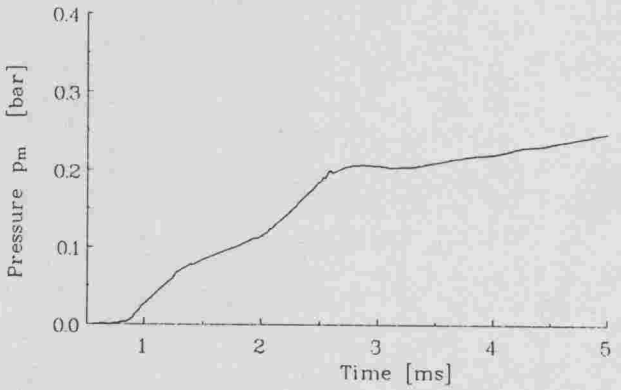

Fig. 9: Pressure within the plenum chamber, $M_\infty = 6.6$, reservoir pressure 380 bar, reservoir temperature 3800 K

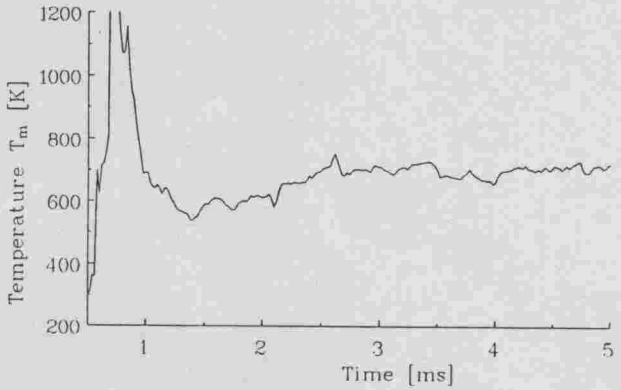

Fig. 10: Temperature within the plenum chamber, flow conditions see Fig. 9

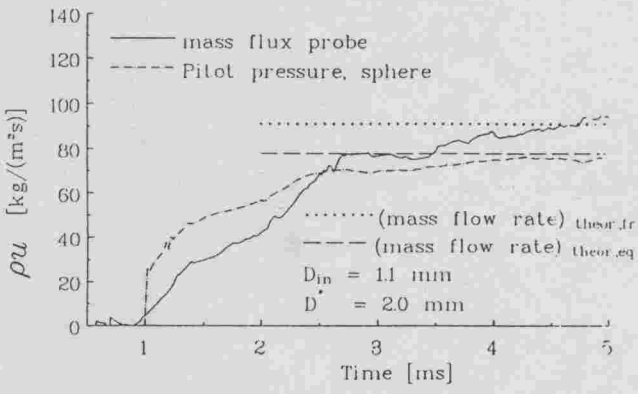

Fig. 11: Free stream mass flux, flow conditions see Fig. 9

The flow inside of the mass flux probe has been computed by Schwane. He used a parallel Navier-Stokes solver for three-dimensional flows [7]. The computational domain is decomposited by the multiblock technique. This is very helpful for the simulation of the cooler, which is placed just between two blocks. In this way the data transfer from one block to the other allows to reduce the total temperature and pressure by an arbitrary amount. Thus the influence of different cooler capacities on the flow can be studied.

Figure 12 shows first numerical results for $M_\infty = 7$, $Re_\infty = 4.2 \cdot 10^5\, m^{-1}$ and $T_0 = 1500$ K. In this case the total temperature behind the cooler was reduced to 1000 K and a total pressure loss of 10 % was assumed for the cooling screens. The same geometry was used as for the probe of Fig. 8.

Figure 12 a shows the Mach number distribution in the whole probe and the decomposition of the computational domain in different blocks.

For this configuration no detached shock occurs, but Figs. 12 a and b show a complex shock geometry at the inlet. The computation gives two large separation bubbles along the diffusor wall. Obviously the wall angle chosen is too large or the throat area of the orifice is too small. By increasing the throat area or decreasing the inlet area the shock system moves inside the diffusor and the pressure rise in the probe is weaker. This would also lead to a smaller separation. But despite of this, the streamline pattern clearly shows that the oncoming free stream at the inlet section is really captured without any disturbances.

Figure 12 c shows a small circulation bubble on the axis just behind the inlet. In the numerical simulation this bubble is due to the vorticity produced by the curved shock near the axis. It is seen that on the axis the shock is not normal. At the moment it is not clear whether this is a real physical effect or a numerical one.

The streamlines in the plenum chamber and through the orifice show no irregular behaviour. In the computation the influence of the cooling screens on the flow has been simulated by a "numerical rake", which is indicated in Fig. 12 c. In this section, which was placed at x = 20, the velocity was set equal to zero at each third grid point in vertical direction.

Despite the fact, that the numerical simulation is not fully equivalent to the real conditions, the computations give very helpful informations about the flow behaviour inside of the probe, which will be taken into account for an improved design.

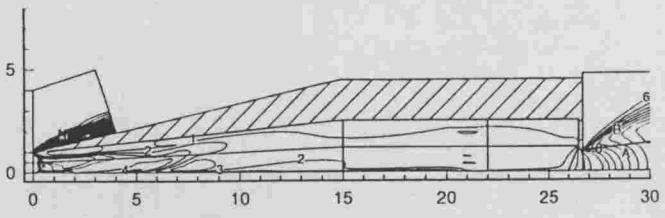

a) Mach number distribution, whole probe

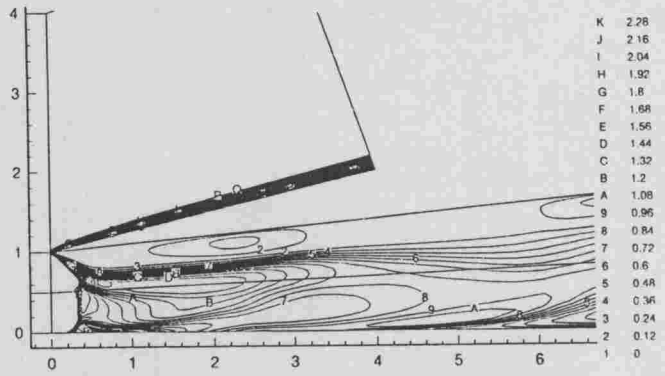

b) Mach number distribution in the inlet area

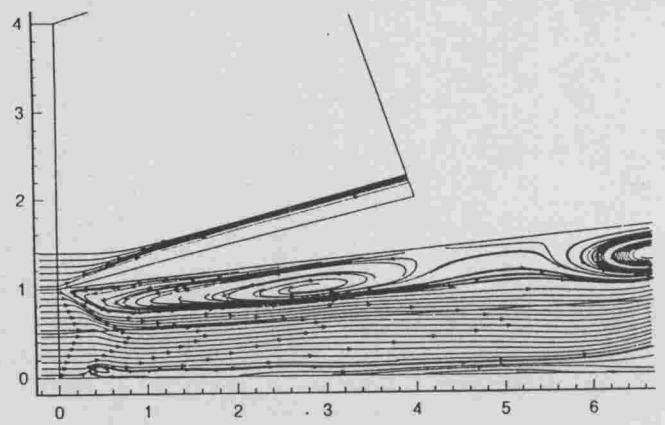

c) Streamlines in the inlet area

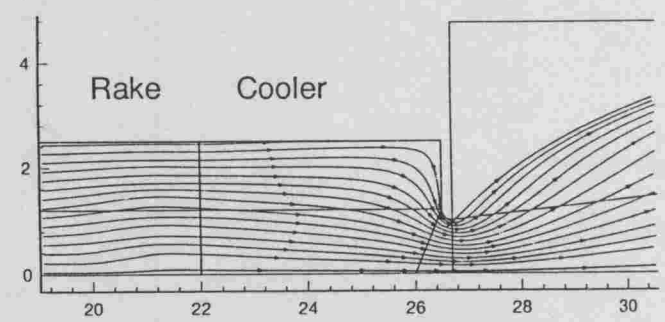

d) Flow through the orifice

Fig. 12: Numerical simulation of the flow inside of the mass flux probe, $M_\infty = 7, Re_\infty = 4.2 \cdot 10^5\, m^{-1}, T_0 = 1500$ K

Measurement of the Free Stream Static Pressure

In sub- and supersonic wind tunnels with different probes the measurement of the free stream static pressure is performed in a more or less routine use. But for hypersonic and especially high enthalpy facilities the application of static pressure probes is not widely spread. During the sixties Nagamatsu [8] performed measurements with a static pressure probe in a shock tunnel and obtained very good results. His probe consisted of a slender tube with a diameter of 12 mm and a small-angle ogive for the nose. The static pressure orifices were placed around the periphery of the probe 260 mm back from the tip. Based on this principle a new probe is under development, where its final diameter will be about 4 mm and its length about 100 mm. The whole design process, which will take into account real gas effects, viscous interaction effects, influence of nose bluntness, etc. is supported by numerical calculations performed by the European Space Research and Technology Center ESTEC, Noordwijk, The Netherlands.

In a first step a big static pressure probe is designed and tested, which allows for the measurement of the pressure distribution along most of its length. The detailed measurements allow the validation of the numerical code, which will be used for the design of the final small probe. The preliminary big probe is shown in Fig. 13.

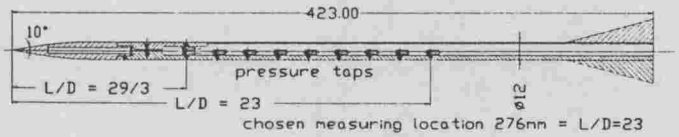

Fig. 13: Dimensions of the preliminary big static probe

It consists of a conical nose with 10° half angle and a transition part to the cylindrical tube of 12 mm diameter. The shape of the transition part is described by a 4th order polynomial, which guarantees continuous second derivative at the junctions to the conical nose and the cylindrical rear part. Ten pressure gauges are placed along the cylindrical part where at the first position 2 gauges are located to check the flow alignment.

For this geometry and different flow conditions Navier-Stokes calculations have been performed by Wong [9]. He used a three-dimensional multi-block Navier-Stokes solver with central and upwind schemes. The upwind schemes consist of finite d ference, symmetric TVD and flux vector splitti For high temperature flows it allows thermo-chemi nonequilibrium modelling.

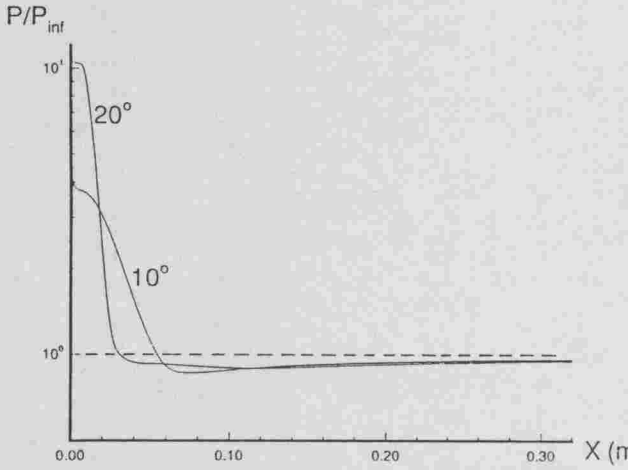

Fig. 14: Pressure distribution along the big sta pressure probe, $M_\infty = 7.2$, $Re_\infty = 4.3 \cdot 10^6\ m^{-1}$, res voir temperature $T_0 = 1500$ K, for two cone angles 10° and 20°

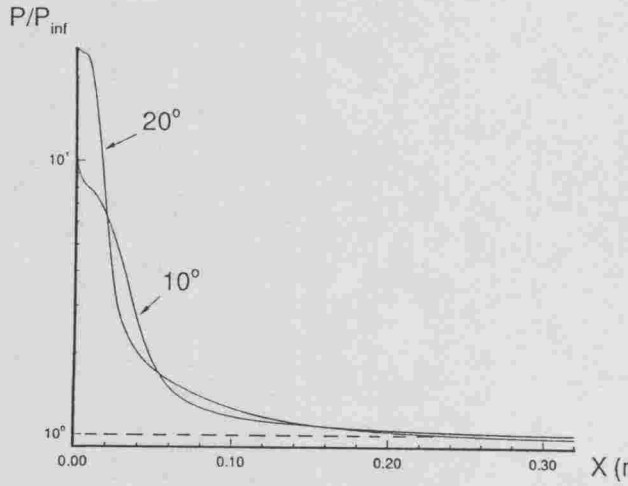

Fig. 15: Pressure distribution along the big sta pressure probe, $M_\infty = 11.3$, $Re_\infty = 1.3 \cdot 10^6\ m$ reservoir temperature $T_0 = 1500$ K, for two cone a gles of 10° and 20°

For two cone angles of 10° and 20° Figs. 14 and show the pressure distribution along the big sta pressure probe, where for the first case viscous int action effects are low and for the second one hig It is interesting to note that for the first case in t nose region an overexpansion occurs and that alo the probe the surface pressure is lower than the fr stream static pressure. In the second case (see Fig. 1 the strong viscous interaction effects avoid the overe

pansion in the nose region and the surface pressure is higher than the free stream static pressure. Computations for high enthalpy conditions show that for the 10° conical nose the shock wave is not strong enough to produce significant real gas effects. Since the static pressure measurement should not be influenced by real gas effects, the cone angle should be as small as possible. Therefore, for the wind tunnel tests a probe with 10° half cone angle has been chosen.

Since for high enthalpy flow conditions it cannot be anticipated that the nose remains ideally sharp, computations with different blunt noses have been performed in order to estimate the influence of a finite nose bluntness on the pressure distribution. First results of these calculations are given in Fig. 16 [9].

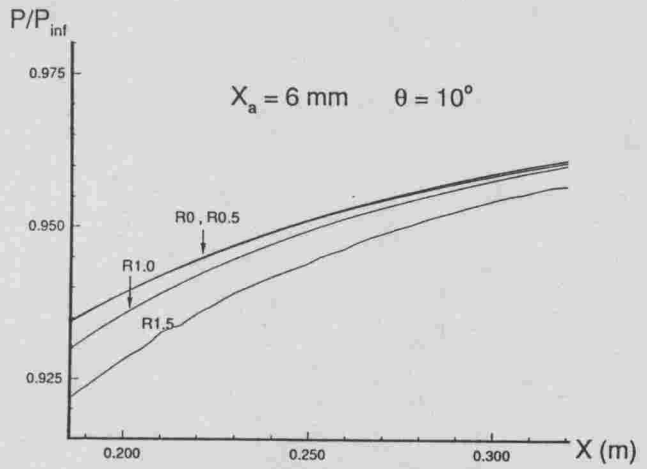

Fig. 16: Influence of a finite nose bluntness on the pressure distribution, $M_\infty = 7.2$, $Re_\infty = 4.3 \cdot 10^6\ m^{-1}$, reservoir temperature $T_0 = 1500$ K,

In Fig. 16 only the results of the rear part of the probe are shown, because only in this region the final measuring location for the static pressure will be located.

From this figure it follows that for a measuring location of x = 276 mm or L/D = 23 for a nose of 1 mm radius the surface pressure is only 0.2 % lower than the sharp nose value, and for a nose radius of 1.5 mm it is 0.7 % lower. This is acceptable, but for increasing nose radius the positive pressure gradient in flow direction becomes larger. This may lead to a flow or at least a boundary layer separation which would give wrong surface pressures. Therefore, by chosing suitable materials it will be tried to fix the nose radius to 1 mm which corresponds to 0.3 mm for the final small probe.

Figure 16 also shows that for a measuring location of 276 mm or L/D = 23 the measured surface pressure deviates from the free stream static pressure only by 5 %. However, for the final geometry computations will be performed for different flow conditions in order to provide a data chart, which takes into account viscous interaction effects, real gas effects, etc. This enables one to determine a correction factor for each flow condition of the form:

$$\left(\frac{p_\infty}{p}\right)_{corr.} = f(M_\infty, Re_\infty, h_0)\,. \qquad (11)$$

The final free stream static pressure follows from the measured and the correction value:

$$p_\infty = p_{meas.} \left(\frac{p_\infty}{p}\right)_{corr.}\,. \qquad (12)$$

As it is anticipated from Fig. 16, the correction factor will be very close to 1.

With the big static pressure probe first tests have been performed, which showed that the probe support, a cone of 30° half angle, was not suitable and produced a huge flow separation. After a modification of the model support to 15° no flow separation occured and the pressure distribution could be measured.

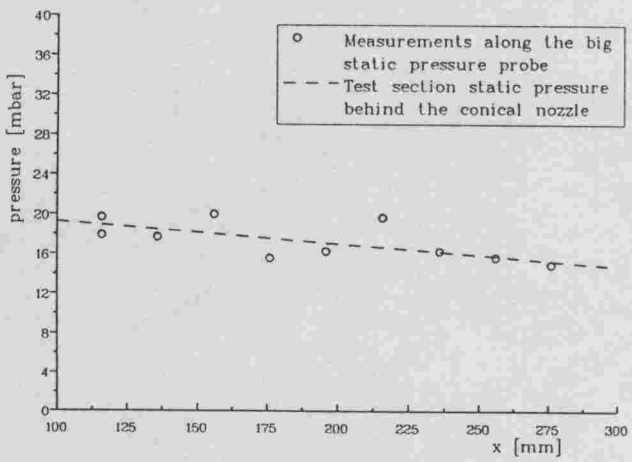

Fig. 17: Pressure distribution along the big static pressure probe, $M_\infty = 6.6$, reservoir pressure 180 bar, reservoir temperature 2700 K

Figure 17 shows preliminary results of the measured pressure distribution along the big static pressure probe. The broken line indicates the free stream static pressure as it is computed from the nozzle reservoir temperature, measured reservoir pressure and measured Pitot pressure. Since the test was performed with a conical wind tunnel nozzle, in downstream direction the static pressure decreases. The pressure gradient was determined by flow field calibration tests. The agreement achieved between the measured static pressure and the nominal value is very good.

FORCE AND MOMENT MEASUREMENTS

Force measurements in short-duration high enthalpy facilities are quite difficult because of the short testing time of one or several milliseconds and the rough test conditions in this kind of wind tunnel. The state of the art of force measurement in short-duration hypersonic facilities was comprehensively reviewed by Bernstein [10]. Since then different approaches were undertaken to measure forces on a model in high enthalpy facilities.

Naumann et al. [11] developed a fast acting release and clamp mechanism, that allows the model to fly freely during the testing time. The accelerations of the model are measured and the forces are derived from the accelerations and the inertia matrix of the model by applying Newtons law: $\underline{F} = \underline{\underline{m}} \cdot \underline{\ddot{x}}$. Problems arise with this technique when the models are small or the forces low, so that not all components of the accelerations can be measured with sufficient accuracy. Also it is not at all easy to determine the inertia matrix of a complicated model that is equipped with six or more accelerometers. This means, that the technique requires an individually equipped model and detailed knowledge about it.

Jessen [12] developed a six component strain gauge balance that was especially designed according to the demands of the Aachen shock tunnel TH2. Its finite element model is shown in Fig. 18.

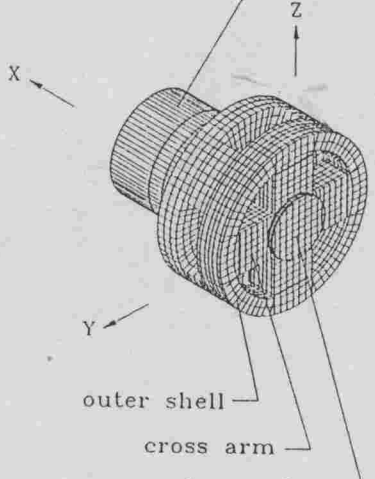

Fig. 18: Finite element model of the balance

The basic idea of the balance is to fix the mode
the model support system via four cross arms, wh
are equipped with semiconductor strain gauges,
on each side of the arm. The deformations of th
cross arms are measured and by a suitable wiring
the gauges the six components can be measured
dependently to a first approximation. All the ot
parts of the structure between model mounting
cross arms only serve to transmit the forces from
model to the cross arms. The center of the cros
connected to the sting via the inner plug by mean
thermal shrinking. The sting itself is connected to
model mounting in the test section of the tunnel.
compact design leads to a high stiffness of the bala
which manifests itself in a high natural frequency.
actly this high natural frequency is needed for a sh
response time, and by this the usefulness of the b
ance for a given application is determined. For
balance described the lowest natural frequency is th
of the pitching oscillations, which roughly amounts
2.3 kHz.

Of course the natural frequency is considerably lo
ered by the inertia of the model. To be sure th
the response time is still sufficiently short, one has
check that the natural frequency of the system mod
balance is not be lower than 1 kHz.

Theoretically a full separation of the six compone
is possible [12], but practically interferences betwe
the components occur. This is primarily due to t
fact, that the center of the cross is not fixed symm
rically to the inner plug but only on one side. The
fore, an accurate calibration is necessary to separa
the six components exactly.

With the comparatively large interferences of t
balance it seems necessary to use a description of t
system taking into account second and third ord
terms, which are necessary to ensure the symmetry
the system for loads acting in the negative directi
[13]. The relation between signal and load is th
given by:

$$S_i = R_{0i} + \sum_{j=1}^{6} a_{ij} Z_j + \sum_{j=1}^{6} \sum_{k=j}^{6} b_{ijk} Z_j Z_k + \sum_{j=1}^{6} c_{ij} Z_j^3 \qquad i = 1, 2...6 \qquad (1$$

with S_i as signal of the strain gauge bridge for com
ponent i, R_{0i} as signal of bridge i without load, Z_j
total load acting on component j, a_{ij} as calibratio
factors for linear terms, b_{ijk} as calibration factors fo
square terms, and c_{ij} as calibration factors for cub
terms.

The calibration factors are calculated from the data of a static calibration by means of a least square fit. The S_i are the measured and digitized quantities during an experiment. As the Z_j are the unknowns, the above nonlinear set of equations has to be solved for each set of six values S_i recorded at a certain instant. This is achieved using the Newtonian method of approximation for a set of nonlinear equations.

The calculated, time dependent forces and moments are transformed from the balance-fixed into the aerodynamic coordinate system and are nondimensionalized with the dynamic pressure and the characteristic dimensions of the model.

First tests with this balance have been performed with a 30° sharp cone model of 200 mm length. There, it turned out that the model sting vibrates with a relatively low frequency and therefore it induces additional forces acting on the balance. These low frequency vibrations are clearly visible in the time history of the lift coefficient in Fig. 19. Störkmann [14] proposed an acceleration compensation method, which eliminates these sting induced forces. The time history of the lift coefficient, corrected in this way, shows no low frequency oscillation and from this data it is quite easy to read a reliable value for the coefficient. The same behaviour is found for the pitching moment.

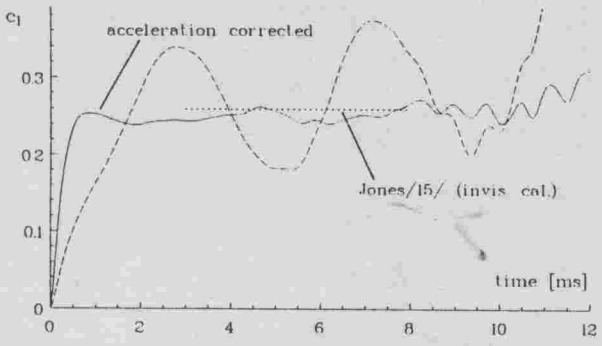

Fig. 19: Time history of the lift coefficient of a sharp 30° cone model, $\alpha = 9°$, $M_\infty = 7.2$, $T_0 = 1500$ K

As expected, the vibrations in the drag component are much smaller (see Fig. 20), but for high angles of attack this will change. For the drag coefficient the acceleration corrected data also show a steadier behaviour than the uncorrected ones. In Fig. 21 the drag coefficient of the cone model is given as function of the angle of attack. There, experimental as well as theoretical values are included. The data obtained by the force balance agree well with other results [16].

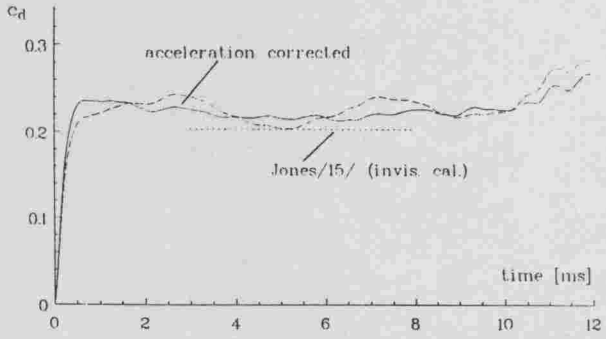

Fig. 20: Time history of the drag coefficient of a sharp 30° cone model

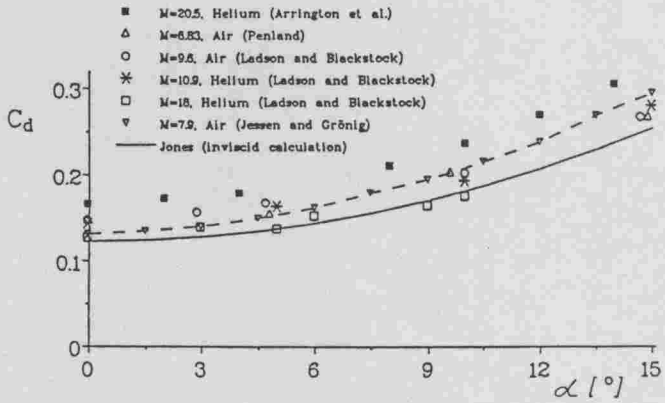

Fig. 21: Experimental and theoretical values of the drag coefficient of a cone as function of the angle of attack

CONCLUSIONS

For shock tunnel applications measurement techniques for surface heat flux measurements have been described. The application of thermocouples for high heat flux regions and of thin film gauges for low heat fluxes for the same model gives an optimum on reliability and accuracy. A coaxial thermocouple has been equipped with a pressure tap, which allows the measurement of heat flux and surface pressure almost at the same location. Flow conditions are determined by a combined Pitot pressure and stagnation point heat flux measurement on a sphere. The method described is quite simple and very accurate over a large region of flow conditions. As a redundant method a probe has been developed, which yields the free stream mass flux. Its advantage is that the principle of the mass flux probe avoids a heat flux mea-

surement at high stagnation temperatures, like it is the case for the stagnation point. Therefore, no problems due to real gas phenomena enter the procedure. But, on the other hand, a suitable probe for short-duration, high enthalpy facilities has to ensure a sufficiently short rise time. For the measurement of the free stream static pressure a probe is under development, which is based on a work of Nagamatsu. The free stream static pressure for hypersonic facilities is not very important to determine the free stream dynamic pressure, mass flux or total enthalpy, etc. But it is very important to characterize the thermodynamical and chemical state of the free stream in high enthalpy facilities, because the free stream static pressure is very sensitive to high temperature relaxation effects. This is the main reason for the development of this probe.

For force and moment measurements a special balance has been developed in order to meet the demands of shock tunnel flows. Work on this balance is still in progress, but the results achieved so far are very promising.

ACKNOWLEDGEMENT

Part of this work was supported by the European Space Agency under contract 11080/94/F/WE. The authors would like to thank Mr. Schwane and Mr. Wong, ESTEC, YPA who performed the computations with great enthusiasm and made a significant contribution to this paper. The authors wish to extend their appreciation to Dassault Aviation, which provided the model for the infrared tests, and to the members of the Shock Wave Laboratory for their work related to this paper and also Mr. B. Schulze who arranged the infrared tests. We also would like to thank Mrs. B. Odenthal for typing the manuscript.

REFERENCES

[1] D.L. Schultz and T.V. Jones, "Heat transfer measurements in short-duration hypersonic facilites", *AGARDograph* no. 165, 1973.

[2] C. Jessen, M. Vetter and H. Grönig, "Experimental studies in the Aachen hypersonic shock tunel", *ZFW, Journal of flight sciences and space research*, vol. 17, no. 2, pp. 73-81, 1993.

[3] J.A. Fay and F.R. Riddell, "Theory of stagnation point heat transfer in dissociated air", *J. Aer. Sci.*, vol. 25, pp. 73-85, 1958.

[4] H. Olivier and H. Grönig, "Influence of the v locity gradient on the stagnation point heati in hypersonic flow", submitted to *Shock Wav*

[5] H. Olivier, "An improved method to determi free stream conditions in hypersonic facilitie *Shock Waves*, vol. 3, no. 2, pp. 129-139, 1993.

[6] R.J. Stalker, "A mass flow probe to use in sh duration hypersonic flows", in W.C. Nelson, *T high temperature aspects of hypersonic flow*. O ford, London, New York, Paris: Pergamon Pre 1964, pp. 271-280.

[7] R. Schwane, "A parallel implicit Navier-Stok solver for viscous hypersonic flows", to be pr sented at *Parallel CFD 95*, CALTECH-Pasad na, June 26-28, 1995.

[8] H.T. Nagamatsu, R.E. Geiger and R.R. Shee "Real gas effects in flow over blunt bodies hypersonic speeds", *J. Aer. Sci.*, vol. 27, no. pp. 241-251, 1960.

[9] H. Wong, *private communication*. Noordwij The Netherlands, 1995.

[10] L. Bernstein, "Force measurements in shor duration hypersonic facilities", *AGRADograp* no. 214, 1975.

[11] K.W. Naumann, H. Ende and H. Mathie "Technique for aerodynamic force measureme within milliseconds in shock tunnel", *Sho Waves*, vol. 1, no. 3, pp. 222-232, 1991.

[12] C. Jessen and H. Grönig, "A new principle for short-duration six component balance", *Exp. Fluids*, vol. 8, pp. 231-233, 1989.

[13] F. Schnabl, "Entwicklung eines Algorithmus zu Auswertung der Eichversuche an 6-Komponen ten-DMS-Waagen", *ZFW, Journal of flight sc ences and space research*, vol. 11, no. 5, pp. 342 346, 1987.

[14] V. Störkmann, *private communication*. Aachen Germany, 1995.

[15] D.J. Jones, "Tables of inviscid supersonic flow about circular cones at incidence $\gamma = 1.4$" *AGARDograph* no. 137, part 1, pp. 1-16, 1969.

[16] C. Jessen, *Messung von Druck, Temperatur und Kraft an Modellen im Stoßwellenkanal*. Doctora thesis, RWTH Aachen, 1993.